Evaluating the use of inertial measurement unit technology during an ice hockey shooting task

Sean Kiyoshi Denroche

Department of Kinesiology and Physical Education

McGill University

Montréal, Québec, Canada

June 2020

A thesis submitted to McGill University in partial fulfillment of the requirements of the degree of Master of Science

Table of Contents

Abstract

This study evaluated the use of a 17-sensor Xsens MVN Link IMU system to measure joint kinematics in comparison to an 18 Vicon camera (4 V5, 4 Vero 2.2, 2 T40S and 8 T10S) optoelectronic system during ice hockey shooting tasks. Ten high-level ice hockey players performed 10 static wrist shots and slap shots on an in-lab artificial ice surface. Concurrent Xsens and Vicon recordings were obtained of each participant's ice hockey shots.

Root Mean Square Error (RMSE) and the Coefficient of Multiple Correlation (CMC) were used to compare the participant's joint angle measures between the two systems. Across all joints, average RMSE were comparable about the X- and Y-axes (within 12°), though RMSE were much higher about the Z-axis. CMC about the X-axis indicated very good curve similarity (0.91), with good (0.78-0.80) and moderate (0.70-0.74) curve similarity observed about the Y- and Z-axes, respectively.

The relative errors observed in this study were predominantly attributed to differences between Xsens' and Vicon's biomechanical models rather than due to differences in technologies. Hence, future research should focus on the standardization of models and calibration procedures, as well as investigate tasks of longer duration and greater complexity. Given the good to moderate agreement between Xsens and Vicon's X and Y axes' absolute measures and measures over time, Xsens is a practical option to quantify representative and real time movement technique of hockey shot skills.

Abrégé

Cette étude a évalué l'utilization d'un système 17-capteurs Xsens MVN Link IMU pour mesurer les kinématiques des joints en comparaison a un système de 18 cameras optoélectric Vicon (4 V5, 4 Vero 2.2, 2 T40S and 8 T10S) durant des lancers de hockey sur glace. Dix joueurs de hockey sur glace de haut niveau ont performé dix lancés du poignet et lancés frappé sur une surface artificielle en laboratoire. Des mesures concurrentes de Xsens et Vicon ont été obtenue pour chaque lancé des participants.

Root Mean Square Error (RMSE) et la Coéfficent de Multiple Corrélations (CMC) ont été utilisés pour comparer les angles de joints des participant entre les deux systèmes. Dans l'ensemble des joints, les RMSE moyenne ont étés comparable dans les axes X et Y (dedans 12°), par contre, le RMSE était beaucoup plus élevé dans l'axe Z. Le CMC dans l'axe X a indiqué une très bonne similarité de courbe (0.91), avec bien (0.78-0.80) et modéré (0.70-0.74) observé dans les axes Y et Z, respectivement.

Les erreurs relatifs observés entre l'Xsens et le Vicon dans cette étude étaits principalement attribué aux differences entre les modèles biomécanique et non aux technologies eux même. Donc, la recherche future devrait concentrer sur la standardization des modèles et les procedures de calibration, ainsi d'enquêter des tâches de longeur durées et de plus grande complexité. Etant donné l'accord de bien à modéré de mesures absolue et en série de temps entre l'Xsens et Vicon dans les axes X et Y, l'Xsens est une option pratique pour quantifier les techniques de mouvements de compétences des lancés de hockey sur glace en temps reels et représentatif.

Acknowledgements

As I write this thesis from the comfort of my home, amid the Covid-19 outbreak, I first want to acknowledge and thank all the frontline workers who have worked tirelessly to keep us safe and healthy throughout this unprecedented time.

I feel very grateful and privileged to have had the opportunity to pursue my academic goals as a member of the Ice Hockey Research Group. I want to thank Dr. David Pearsall for granting me this opportunity and allowing me to learn and develop as researcher and as a person. I also want to thank Dr. Pearsall for encouraging me and trusting me with learning a new system and taking on this project. To our research assistant Philippe Renaud; thank you for all your support throughout the last two years. The completion of this project would not have been possible without you. I would also like to thank Dr. Shawn Robbins for his expertise and support throughout the analysis of my data. To my lab mates; thank you for all your support and friendship. I always enjoyed coming into the lab every day because of the great group we had. To Aimée Quintana, thank you for all your help and positivity when learning the new system together. To Matt Kelly, thank you for all your help with data collection and processing. To Dr. Stacey Acker from the University of Waterloo, I want to thank you for giving me the opportunity to get involved in biomechanics research as a second-year student. Your support and guidance throughout my undergrad degree and undergrad thesis have been incredibly vital to my development and preparation for grad school and my future endeavours.

To the boys back home, I thank you all for always being there for me and always providing a positive distraction when I needed it. Our virtual hangouts over the last two years have meant more to me than you may think. To Hoang-Nghi Dam-Le, thank you for everything. Despite it being in another city, you encouraged me to pursue this opportunity and have

supported me endlessly throughout it. Your patience and love throughout the last few years have been incredible and I am so lucky to have you by my side. Lastly, I want to thank my family. I am so grateful for every opportunity you have provided me from falling in love with the sport of hockey to moving to Montreal to research it at the Master's level. Thank you for all your unconditional love and support.

Contribution of Authors

Sean K. Denroche, MSc. Candidate, Department of Kinesiology and Physical Education, McGill University, was responsible for the research design, collection of data, processing and analysis of data and the writing of this thesis. The candidate's supervisor, David J. Pearsall, PhD, Associate Professor, Department of Kinesiology and Physical Education, McGill University, contributed to the research design and analysis of the data.

Shawn Robbins, PhD, Assistant Professor, School of Physical and Occupational Therapy, McGill University, helped develop the data processing pipelines and aided with the statistical analysis. Dr. Robbins was also a member of the thesis advisory committee alongside Dr. Richard Preuss, Assistant Professor, School of Physical and Occupational Therapy, McGill University. Philippe J. Renaud, MSc., Department of Kinesiology and Physical Education, McGill University, played a very important role in the research design, data collection and data analysis, acting as the lab research assistant.

Aimée Quintana, MSc. Candidate, Department of Kinesiology and Physical Education, McGill University, played a critical role in developing our understanding of the Xsens system. Finally, Matthew Kelly, MSc. Candidate, Department of Kinesiology and Physical Education, McGill University, aided in data collection and data processing.

List of Tables

List of Figures

1. Introduction

Biomechanical research relies heavily on the use of technology and instrumentation to collect data. With regards to recording human body joint kinematics, three-dimensional motion capture by means of multi-camera optoelectronic systems within a fixed, delimited field of view laboratory conditions has been viewed as the gold standard to estimating these measures with high accuracy. Unfortunately, for rapid, complex and unpredictable human movement skill sequences that occur over large fields of view and with multiple subjects, optoelectronic systems are impractical. This is especially the case for sport and exercise biomechanics research where the ideal environment to capture data in is the expansive environments where an athlete trains and competes. In sports such as ice hockey, capturing detailed quantitative movement data without sacrificing the natural dynamics has been challenging.

An alternative, potential technological solution is to adopt advanced inertial measurement units (IMUs) to track subject's body movements. IMUs are wearable sensors containing an accelerometer, magnetometer and gyroscope that can be used to measure segment kinematics without the required lab-camera set-up. Wearable IMUs have been shown to be practical and accurate for occupational assessment, gait analysis and some sport contexts. The potential of IMUs to evaluate whole-body kinematics in ice hockey has not been studied extensively, in particular, for stick and shot related skills. Hence, the purpose of this study was to evaluate the use of a commercial IMU system to record whole-body kinematics during ice hockey shooting tasks. If successful, future validation of this technology will expand the possibilities of data collection in future ice hockey research to aid athlete and coaching skill development.

2. Review of Literature

2.1 Human Motion Capture and Analysis

Human body and segment motion capture is a commonly used tool within the study of biomechanics. The evolution of this technology has been critical in the advancements in our knowledge of kinematics: the study of motion without referencing the forces that influence that motion (Oatis, 2017). One of the earliest examples of motion capture was in 1872 when Eadward Muybridge used cameras to photograph a series of images of a horse's trot in order to determine whether there was ever a point in time when the horse had no hooves on the ground (Baker, 2007). Concurrently, Jules-Étienne Marey developed camera shutter techniques that allowed him to use a single photographic plate to capture several images, known as the chronophotograph (Baker, 2007). In the late 1800's, walking gait was quantitatively analyzed in terms of body segment and joint kinematics by Otto Fischer and Willhelm Braune. During this analysis, Geissler tubes were used to illuminate the segments of the body and were strapped to the participant. The participant was then instructed to walk in the dark while images were captured using a camera with rotating shutter opening intervals. Fischer and Braune then measured points on these images and used these point coordinates to calculate joint centres and eventually joint moments (Baker, 2007). The work of Muybridge, Marey, Fischer and Braune highlights the early developments of motion capture research made possible by various scientists, mathematicians and photographers. With the introduction of computer tracking tools, the development of today's modern and practical motion capture systems became possible.

Measuring human kinematic data may be achieved through a variety of different technologies, ranging from a simple goniometer, electromagnetic sensors or optoelectronic camera systems. Electromagnetic systems can track spatial position of sensors without need for

visible line of site in contrast to optoelectronic systems. Electromagnetic systems are limited, however, with respect to the sensors' sensitivity to ferromagnetic materials, the presence of noise in the signals and the sensors' limited range that can decrease the accuracy of the data (H. M. Schepers & Veltink, 2010). In general, optoelectronic systems outperformed all electromagnetic systems in terms of data accuracy (Eline van der Kruk & Reijne, 2018). An optoelectronic system uses a fixed camera set-up to determine the position of a marker in three dimensional space. In passive systems, the cameras emit and detect infrared light that reflects off of the markers. In contrast, active systems use markers that emit infrared light pulses detected by the cameras. Optoelectronic systems have become the standard reference for motion capture validation (Bidabadi, Murray, & Lee, 2018; Robert-Lachaine, Mecheri, Larue, & Plamondon, 2017b; Seaman & McPhee, 2012). Despite their popularity, optoelectronic systems are limited primarily to lab settings for with a fixed multicamera set-up, and the need for constant marker visibility (Bidabadi et al., 2018; Eline van der Kruk & Reijne, 2018).

2.2 Inertial Measurement Units (IMU)

Optoelectronic systems lack the portability and field of view required to be practical for the analysis of sport skills, thus; researchers have recently explored the potential of inertial measurement units (IMU) to track body movement. IMUs are small sensors that can be easily attached to and removed from different segments of the body or to an instrument or piece of equipment (Bidabadi et al., 2018; Seaman & McPhee, 2012). These lightweight sensors are wearable and require lower energy usage (De Vries, Veeger, Baten, & Van Der Helm, 2009; Taylor, Miller, & Kaufman, 2017). A single IMU sensor is typically comprised of an accelerometer, a magnetometer and a gyroscope, sensitive to movements in the X-, Y- and Z-axes respectively (Bidabadi et al., 2018). Forward navigation algorithms (e.g. Kalman filters) are

used to fuse data from these three sensors to determine sensor angular velocity, acceleration and orientation (Eline van der Kruk & Reijne, 2018). IMU systems, however, are susceptible to drift error in global position and distorted signals near ferromagnetic materials (Eline van der Kruk & Reijne, 2018). Consequently, optoelectronic systems' accuracy are often used to validate the use of IMU systems in new environments or contexts (Robert-Lachaine et al., 2017b).

2.2.1 Xsens MVN System

Xsens (Enschede, Netherlands) is one of the leading manufacturers of IMU technology. The Xsens system consists of 17 IMU sensors that are attached along the whole body that communicate wirelessly to an access point. Each sensor contains a three-dimensional gyroscope, a three-dimensional accelerometer and a three-dimensional magnetometer (H. Schepers, Giuberti, & Bellusci, 2018). The tri-axial gyroscope is used to capture angular velocity, while the accelerometer measures the acceleration based on the gravitational force of the earth. Finally, a magnetometer provides yaw (heading) orientation based on the earth's magnetic field. These three sensors' signals are fused by way of Kalman filter algorithms, to estimate body segment position and trajectory. From the 17 IMUs, the MVN Analyze software builds a 23-segment virtual model used for visual animation and data analysis (see Section 4 for more details).

2.3 IMU Validation

Given the rapid development of wearable smart sensor technologies, IMUs have become more common in the field of biomechanics research. Each IMU system must be validated in terms of their ability to accurately track body movement. For example, Taylor et al. (2017) used a motorized dynamic arm to move an IMU sensor (Opal version 2, APDM Inc., Portland, USA) through known angular displacements and velocities. Controlled angular displacement and velocity movements were tested. These IMUs demonstrated sufficient accuracy (within 0.6° for

static, 4.4° for dynamic) with small angular displacements and at low angular velocities during the dynamic testing (Taylor et al., 2017).

More recent studies have explored IMU accuracy for tasks of greater complexity and duration (Robert-Lachaine et al., 2017b). For example, Kim and Nussbaum (2013) compared the Xsens MVN system to the Vicon MX optoelectronic system's estimates of joint kinematics and moments during five different manual materials handling (MMH) tasks over an extended period of time. They reported this IMU system to be relatively stable over time; however, mean and peak absolute error was task-dependent with greatest error observed during larger or whole-body movements and more pronounced during the later testing phases. Overall, however, the data collected by the IMU system was found to be more affected by the task complexity rather than the time (Kim & Nussbaum, 2013).

In a similar study, Robert-Lachaine et al. (2017b) compared an Xsens MVN system and Optotrak optoelectronic system (Northern Digital, Waterloo, Canada) during a series of MMH tasks, taking into account task complexity and duration. Twelve participants were instructed to move empty boxes between four platforms. It was concluded that the technology data differences (optoelectronic vs IMU) were relatively low whereas large discrepancies between respective biomechanical models were observed (Robert-Lachaine et al., 2017b). With respect to task complexity and duration, a higher root mean square error was associated with longer and more complex tasks (Robert-Lachaine et al., 2017b). These results were supported from prior studies that also found that IMU performance with respect to accuracy was dependent on task complexity (Brodie, Walmsley, & Page, 2008; Godwin, Agnew, & Stevenson, 2009; Plamondon et al., 2007).

The feasibility of *in situ* task analysis is promising for sport, rehabilitation and gait analysis research (Robert-Lachaine et al., 2017b). For example, Bidabadi et al. (2018) studied the use of an IMU system (built in-house) to measure foot pitch angle during walking in comparison to a Vicon optoelectronic system. Participants were tasked with walking in a straight line while RMSE and correlation measurements of foot pitch angle measurements were compared between the two systems. A mean correlation of 99.5% was calculated, with a standard deviation of 0.834%, while the RMSE between the two systems was found to be low, 1.6-3.7° (Bidabadi et al., 2018). Ferrari et al. (2010) conducted a study comparing the use of Xsens and Vicon systems during different gait analysis protocols. Ferrari et al. (2010) also performed multiple comparisons including an analysis comparing the two technologies. Quantifying curve similarity using the coefficient of multiple correlation (CMC), very good or excellent similarity was found in all lower limb joints (Ferrari et al., 2010). The CMC measurement used in this study has also been adopted by multiple comparative studies (Lee, Laprade, & Fung, 2003; Mayagoitia, Nene, & Veltink, 2002; Robert-Lachaine et al., 2017b). For example, J. T. Zhang, Novak, Brouwer, and Li (2013) used CMC to compare an Xsens system to an optoelectronic system during level walking and walking up and down stairs. Excellent CMC values (CMC > 0.96) were observed in the sagittal plane, while these values decreased in the other two planes. J. T. Zhang et al. (2013) attributed potential differences to discrepancies in the anatomical frames used by the two systems.

With regards to running tasks, Wouda et al. (2018) compared treadmill running kinematics using an Xsens IMU system and optoelectronic system and Plug-In Gait marker set-up. The ankle, knee and hip joint kinematics were analyzed in all three axes. Comparison across the two systems showed a strong correlation for joint angles in the sagittal plane, however

greater differences were observed for the frontal and transverse planes (Wouda et al., 2018). These discrepancies were consistent with other literature (Robert-Lachaine, Mecheri, Larue, & Plamondon, 2017a; H. Schepers et al., 2018). In a similar study, H. Schepers et al. (2018) collected joint angle data during treadmill running and over ground walking in order to compare the Xsens MVN system to OpenSim software (Stanford University, Stanford, USA). In general, RMSE for the hip, knee and ankle were all comparable but with slightly lower amplitudes in the sagittal plane in comparison to the frontal and transverse planes. Additionally, two different calibration procedures were implemented including the Xsens N-pose and a static pose obtained from OpenSim. When applying the OpenSim calibration to the data, RMSE values were found to decrease (H. Schepers et al., 2018).

2.4 IMU Validation Studies in Sports

2.4.1 IMU Validation Studies in Sports

Other than gait analysis studies involving walking and running, few studies of other sport activities have compared IMU motion tracking to optoelectronic or video based systems. Krüger and Edelmann-Nusser (2010) conducted a validation study for the Xsens IMU system in alpine skiing. The IMU system was compared with a video based optical system and the two systems were found to be highly correlated. Despite promising results, the authors noted that the performance and accuracy of the system may vary depending on the conditions, such as the snow quality's effect on skiing speed. Nevertheless, it was concluded that an IMU system was a very useful tool in sports such as alpine skiing where an unrestricted capture area is necessary (Krüger & Edelmann-Nusser, 2010). Another sport-related validation study from Fulton, Pyne, and Burkett (2009) used an IMU system (MiniTraqua™, version 5, Cooperative Research Centre for Microtechnology, Australian Institute of Sport) to measure leg kick count and rate during

freestyle swimming and kicking-only swimming. IMU and underwater video-based results were compared. A correlation of 0.96 and 1.00 was found between the two systems for the freestyle and kicking-only swimming styles, respectively. Overall, they concluded that the IMU system was both valid and reliable and that other swimming strokes should be investigated in order to implement the technology in coaching and biomechanical performance enhancement (Fulton et al., 2009). In tennis, Ahmadi, Rowlands, and James (2010) used inertial sensors (Kionix Inc., Ithaca, USA) to measure the angular velocity of the upper arm during tennis serving. Results showed that the IMU sensors' data were consistent with that of the reference video records. As a final study example, Koda et al. (2010) examined baseball pitchers using inertial sensors placed on the upper arm and forearm in comparison to an optoelectronic system. Joint kinematics of the upper limb were recorded by the sensors and were found to have a strong correlation (> 0.90) with those captured by the optoelectronic system.

In addition to the above, IMUs have been explored for the analysis of sports equipment. For example, Seaman and McPhee (2012) compared the tracking of golf club swings using both an IMU system and an optoelectronic system. In brief, the two systems were very comparable when tracking the orientation of the golf club; however, large differences were observed with respect to the club's position. This is consistent with other reports wherein IMU systems have difficulty with tracking position as a stand-alone system (Eline van der Kruk & Reijne, 2018). Another equipment-based study and, to our knowledge, one of the few published studies using an IMU system in ice skating was published by E van der Kruk, Schwab, Van Der Helm, and Veeger (2016). The purpose of this study was to validate measurements of the lean angle of the skate using IMU-based skating stroke detection. A klapskate was instrumented with an IMU as well as reflective markers to be tracked by the optoelectronic system reference. The two systems

were used to track the orientation of the skate to better understand the push-off phase of the skating stride. The IMU system provided a reliable measurement of the skate's lean angle, suggesting that it can provide useful performance feedback to skating athletes (E van der Kruk et al., 2016). While these validation studies show promising results with respect to implementing IMU systems in *in situ* biomechanical sports research, numerous researchers have applied this technology to studies analyzing movements and providing performance feedback for athletes.

2.4.2 Examples of IMU use for Movement Analysis in Sports

Collecting movement analysis data in athletes in their natural environments has become feasible with IMU's. For example, Ahmadi et al. (2014) used IMU sensors for the purpose of movement analysis during different tasks such as running, box jumps and agility cuts. Acceleration and orientation data from the knee and hip were compared using a discrete wavelet transform and machine learning were able to classify the different activities with 98% accuracy. (Ahmadi et al., 2014).

As another example, a study of marathon running demonstrated the use of IMU technology to analyze movement in a sport specific environment (Reenalda, Maartens, Homan, & Buurke, 2016). Three marathon runners wore Xsens IMU sensors during a full 42.2 km marathon. As the participants ran, data from the sensors were transferred to receivers transported by bicycle within range of the sensors. Lower body kinematic parameters, such as maximum hip and knee angles, were measured at different phases of the running gait cycle throughout the race. This study evaluated how the lower body kinematics changed throughout the race. Significant differences in lower body running mechanics between the early and late stages of the race were identified. Although the study was limited by sensor battery life and sample size, the feasibility

of conducting an extended analysis of movement in a sport specific environment was displayed (Reenalda et al., 2016).

2.4.3 Examples of IMU use for Sport Performance Feedback

In golf, technological tools have been used to provide athletes and their coaches with sport specific feedback on their swing in relation to shot performance. For example, Ghasemzadeh, Loseu, and Jafari (2009) used sensors embedded with tri-axial accelerometers and bi-axial gyroscopes to track wrist rotation during golf swings. Sensors were placed on the golf club (one by the club head and one by the gripping region), and the athlete's right wrist, left arm and waist. The data from these sensors were used to model the golf swing with respect to wrist movements in order to provide useful feedback for golfers (Ghasemzadeh et al., 2009). A similar feedback-oriented study detected ball contact and kinematic parameters during golf putting (Jensen et al., 2015). A golf putter was instrumented with a single IMU sensor containing a tri-axial accelerometer and tri-axial gyroscope. They developed a system that could detect when a putt had occurred and provide feedback with respect to kinematic parameters such as the duration of the putt, club head angle and angular velocity at ball impact. Similar to Ghasemzadeh et al. (2009), this IMU-based system was designed to provide useful feedback to help train golfers and keep track of learning progress (Jensen et al., 2015).

Bächlin and Tröster (2012) used accelerometer sensors placed on the wrist and back to develop a feedback system to evaluate athlete swimming performance. An algorithm was developed and used to calculate performance variables from IMU signals such as swim velocity and distance per arm stroke. This study demonstrated the feasibility of using wearable sensors to provide feedback on specific parameters that are difficult to assess from a coach's perspective outside of the water (Bächlin & Tröster, 2012).

In summary, the above studies exemplify the growth of interest and feasibility of adopting IMUs in the context of different sports, and how they can enhance the training of elite athletes in their natural training or competition environments.

2.5 Current State of Ice Hockey Research

Ice hockey biomechanics research has primarily focused on the two main pieces of equipment, skates and sticks, and their respective tasks: skating and shooting. With respect to sticks and shooting, previous research has focused on the material and design properties of the stick, as well as techniques of the two most common types of the shots: the wrist shot and the slap shot. For example, Pearsall, Montgomery, Rothsching, and Turcotte (1999) examined the effects of stick shaft stiffness on slap shot velocity. Four different sticks of varying stiffness were compared during slap shots within a lab setting. Puck velocity was measured using a radar gun, while stick deformation was captured using a high-speed camera. The differences in puck velocity across stick types were relatively small, while greater variability was seen between participants. This study suggested that shot quality was more dependent on player behavior than stick stiffness. Similar results were reported by T.-C. Wu et al. (2003) comparing puck velocity between skilled and unskilled players for both wrist and slap shots. Similarly, stick stiffness did not appear to affect shot velocity, whereas, player technique and individual strength factors were more relevant (T.-C. Wu et al., 2003). In comparison, Worobets, Fairbairn, and Stefanyshyn (2006) found that stick stiffness also had no effect on slap shot velocity but had some influence (50% variance) on wrist shot velocity. The way the player loads the stick, to store elastic potential energy, was considered to have more influence on shot velocity (Worobets et al., 2006).

In addition to studying the material properties of sticks, a few ice hockey shot technique and execution studies have been done. Michaud-Paquette, Pearsall, and Turcotte (2009)

examined the important mechanical predictors of wrist shot accuracy. This study consisted of 25 subjects performing stationary wrist shots in a lab environment. The kinematics of the stick's shaft and blade, as well as the puck, were measured via an optoelectronic system. Several variables were examined such as blade orientations, shaft bend, puck velocity at release. Multiple regression analyses were then used to determine which variables best predicted the accuracy of the shot. A subsequent study examined the whole-body kinematic predictors of wrist shot accuracy (Michaud-Paquette, Magee, Pearsall, & Turcotte, 2011) using whole-body kinematics of participants derived from optoelectronic motion capture. Multiple regression analyses were used to determine the variables most related to shot accuracy. In summary, the analysis of whole-body, stick and puck kinematics can provide useful information in understanding the motor control strategies necessary for an accurate wrist shot performance (Michaud-Paquette et al., 2011). Such information provided in real-time would have valuable coaching applications.

Despite the recent advancements made in our understanding of ice hockey biomechanics, most of the previous research has been limited to simulated ice surfaces within a laboratory environment. Recent work prior to 2017 was conducted on an artificial ice surface in a lab environment with limited space. As such only stationary wrist shots and slap shots have been studied precluding game intrinsic concurrent skating and shooting dynamic movements common in ice hockey.

To address this limitation, Renaud et al. (2017) recently demonstrated the feasibility of collecting 3D motion capture data on ice to study the lower body kinematics of ice hockey skating starts. In comparison to the previous research, the results of on-ice data collection provided comprehensive insight into factors affecting skate start performance (Renaud et al., 2017). The ability for testing *in situ* within the ice arena environment and to capture movements

over a greater area demonstrated the feasibility and coaching translatable value of their results. This subsequently led to further on-ice studies: Shell et al. (2017), Budarick et al. (2018) and Robbins, Renaud, and Pearsall (2018) have since published research on ice hockey skating biomechanics using data collected on-ice.

One drawback to the on-ice data collection, however, is the logistical challenge of camera set-up: unless a permanent set-up is available, the repeated set-up and take down of cameras and equipment between data collections is labour intensive and time consuming (Renaud et al., 2017). Furthermore, unless the cameras can be mounted off the ice, the feasibility of capturing data in an actual game or game-like scenario remains in question due to the caution that must be taken to avoid damaging equipment.

Hence, an on-ice data collection method that would not require the labour intensive set-up of an optoelectronic system would be the use of wearable IMU sensors. The feasibility of using IMU technology in lieu of optoelectronic motion capture has been demonstrated in the aforementioned validation studies in various ergonomic and sport contexts. Furthermore, IMU technology has shown promise in sport-specific studies analyzing movement patterns and providing feedback. For example, in an on-ice specific example, E van der Kruk et al. (2016) demonstrated the use of IMU-instrumented klapskates to study the push-off phase in speed skating. As an example in ice hockey, past studies investigating sticks and shooting have demonstrated the feasibility to embed accelerometers in the puck to obtain performance specific measures of shooter technique (Lomond, Turcotte, & Pearsall, 2007; Villaseñor, Turcotte, & Pearsall, 2006). Most notably, Whiteside, Deneweth, Bedi, Zernicke, and Goulet (2015) used an Xsens IMU system to measure hip mechanics in ice hockey goalies in a study investigating the development of femoro-acetabular impingement. Whiteside et al. (2015) demonstrated the

feasibility of using the Xsens system in a study where the use of an optoelectronic system would not be possible due to the marker occlusion caused by goaltender equipment. Thus, IMU technology shows promise in analyzing whole body kinematics in ice hockey.

3. Objectives and Hypotheses

Adopting IMU technology in ice hockey movement skill evaluation may enhance the efficiency in data collection and rendering (i.e. real time; making it practical for training and coaching use) as well as bring the “lab to the ice” to offer externally valid measures of performance within the actual expanse of the ice hockey arena. Adoption of IMU technology in ice hockey would save time and financial resources and may increase the quality of research conducted. However, the verification of IMU measurement accuracy for body and stick motion in selected ice hockey skills is warranted.

Hence, the objective of the proposed study is therefore to evaluate the use of a commercial IMU system (Xsens, Enschede, Netherlands) to capture whole-body kinematic data during an ice hockey shooting task. The kinematic data captured by the Xsens system will be compared against the data captured by a Vicon optoelectronic system, which will act as a reference standard. The measurement error and curve similarity between the data measured by the two systems will be assessed during static shooting tasks in an in-lab environment.

Similar to previous IMU validation studies, it is hypothesized that the Xsens system will perform with greater accuracy when measuring joint angles within the sagittal plane in comparison to the frontal and transverse planes. Furthermore, due to the dynamic nature of the task being measured, it is hypothesized that the observed measurement error in this study may be greater than what has been reported in other studies. Lastly, it is hypothesized that marginal temporal effects on measurement error may be present, resulting in greater error in the later phases of data collection sessions.

4. Methods

4.1 Participants

Ten ice hockey players participated in the current study. Participant playing levels ranged from junior to university ice hockey; all participants had played hockey in the past calendar year and were free of serious injuries at the time of data collection. Descriptive statistics for the participants are given in Table 1. Prior to data collection, testing procedures were explained in written and oral format to the participants, who then signed an information and consent form in accordance with the Tri-Council Policy Statement on Ethical Conduct for Research Involving Humans (McGill REB II, File #: 375-0216).

Table 1 Descriptive statistics of participants.

Age (yrs) mean ± SD	**Height (m)** mean ± SD	**Weight (kg)** mean ± SD	**Experience (yrs)** mean ± SD
26.70 ± 5.0	1.8 ± 0.1	87.6 ± 7.9	21.3 ± 3.8

4.2 Testing Instrumentation

4.2.1 Vicon Optoelectronic Motion Capture

A Vicon optoelectronic system (Vicon, Oxford, UK) was used as a standard reference of comparison to the Xsens MVN Link system. The Vicon system consisted of 18 cameras: 8 T10S, 2 T40S, 4 Vantage V5 and 4 Vero 2.2 cameras recording at a sampling rate of 240 Hz. The cameras were mounted on tripods at various heights surrounding the capture area and were connected to an MX Giganet connection Hub and desktop computer. The camera positions remained consistent throughout the entire data collection. The in-lab motion capture volume's dimension was approximately 8.0 m long x 3.4 m wide x 2.0 m high, described in more detail in Section 4.3. 52 retroreflective spherical markers (14 mm diameter) were placed on the

participant in accordance with an adapted version of the Plug-in Gait full body model (Nexus 2.6, Vicon, Oxford, UK), Figures 1 and 2. The single forearm marker was replaced by a cluster of four markers with medial and lateral forearm markers placed distal to that cluster. The wrist and hand markers were replaced by clusters of five markers placed on each hockey glove worn by the participants during data collection. Foot marker placement remained the same; however, these markers were placed on the exterior of the ice hockey skates worn by the participant. An additional four markers were placed on the puck, ten markers were placed along the stick's shaft and blade and eight markers were placed along the posts and cross-bar of the net. These markers were used primarily for event detection calculations in post data processing. Pre-testing for the Vicon system involved a palms-down, forward-elbows bent static calibration pose held by each participant for five seconds. This calibration was done to expose all markers to determine the model of each participant's initial coordinate system's reference frame.

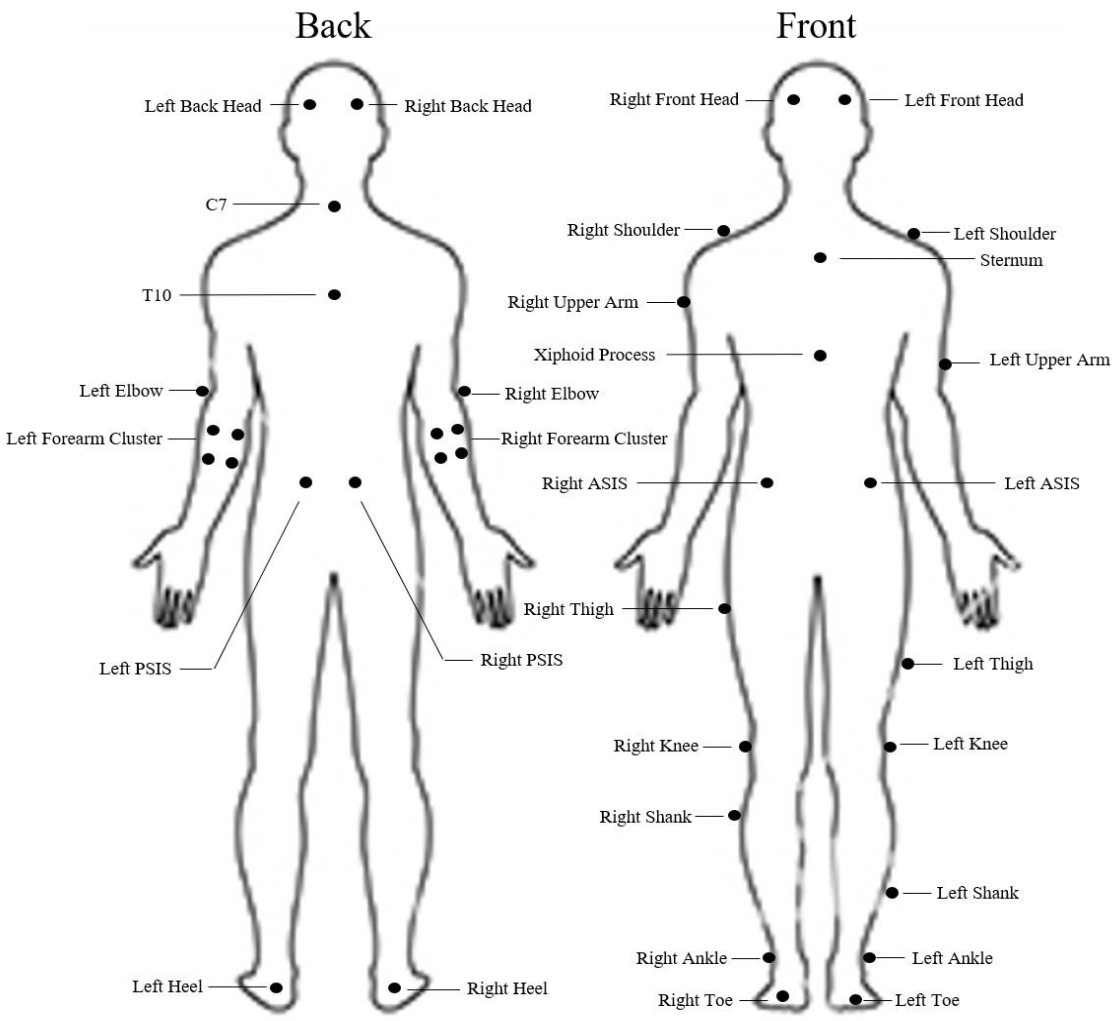

Figure 1 Reflective marker placement in adapted Plug-in Gait model.

Figure 2 Reflective marker placement on gloves, stick and puck. Markers on the stick are indicated by the red arrows.

4.2.2 Xsens IMU Motion Capture

The Xsens MVN Link system (Xsens, Enschede, Netherlands) was the Inertial Measurement Unit (IMU) system used for this study. The MVN Link system consists of 17 IMU sensors connected through wires about the entire body. Sensors were placed on the head, pelvis, sternum and along all four limbs of the body, as seen in Figure 3. Through the wire leads, the sensors communicate vis-à-vis to a "body pack" worn on the participant's back that in turn communicates using a Wi-Fi connection access point. Like the Vicon system, the MVN Link system captured data at a sampling frequency of 240 Hz. The indoor office and outdoor/indoor open space range for data capture is reported to be 50 m and 150 m, respectively (Xsens, 2018), greatly exceeding the typical capture volume of an optoelectronic system. The Xsens system must also be calibrated prior to data collection. This calibration process required the participant to stand in a static N-pose (neutral posture) or static T-pose (arms out 90° to the side, and palms down) for approximately 4 seconds before walking in a straight line forward for approximately 10 m, then walking back to the origin to resume the static posture. Xsens then will indicate the

quality of calibration which may result in “good”, “acceptable”, “poor” or a failed calibration. The N-pose was used, as recommended by the manufacturer (Xsens, 2018) and only “good” calibrations were accepted during this study. The Xsens MVN software provides different “scenarios” to choose from that are mainly dependent on the way the user interacts with the floor of the environment. The “No-Level” scenario, where the user’s avatar is fixed in one global position at the pelvis, was selected for this study. This scenario was best for studies that were not concerned with global positioning or environmental interactions. Furthermore, this scenario was best suited for tasks such as skating where, unlike walking or running, contact events between the foot and the ground are not well defined (H. Schepers et al., 2018).

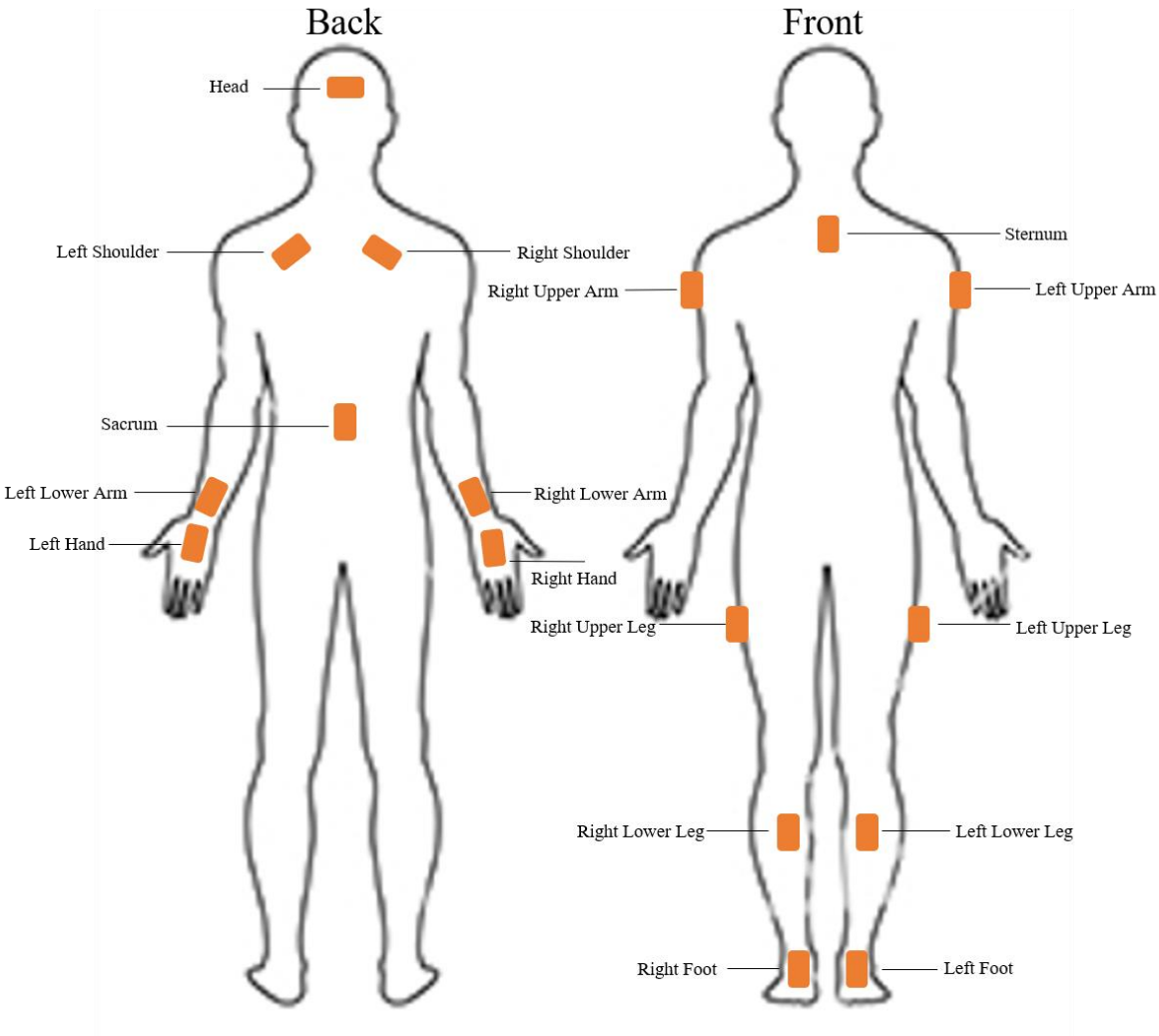

Figure 3 IMU sensor placement in accordance with Xsens MVN model.

4.3 Testing Protocol

In-lab testing allowed for the evaluation of the Xsens system in a controlled and optimized environment prior to its use on-ice. This environment ensured strong marker visibility and high data quality captured by the Vicon cameras to serve as a reference. Furthermore, the fixed and dedicated in-lab set-up allowed for the collection of a large amount of trials in a shorter period of time. The testing took place in the Ice Hockey Research Lab at Currie Gymnasium on

campus at McGill University in Montréal, Québec. The 18 Vicon cameras were placed around a synthetic ice surface (Viking, Toronto, Canada) of dimensions 3.4 m wide x 8 m long (Figure 4).

Prior to testing, a participant's body anthropometrics were measured as necessary for the respective three-dimensional models associated with the Xsens and Vicon systems (see Table 2). Subsequently, the Xsens system was mounted on the participant. The Xsens sensors were secured to the body using double-sided tape placed between the sensor and participant's skin, with additional medical tape placed over top of each sensor for security. This process was used for all sensors with the exceptions of the hand sensors (worn via gloves), head sensor (placed inside of a headband) and the foot sensors (taped exterior to boot laces). With sensors in place, the participant put on a tight fitting Xsens T-shirt that contained pockets for the Xsens body pack, battery pack, and sensors' wires. In addition, the participant was fitted with a full-body, tight fitting Velcro suit (OptiTrack, Corvallis, USA). Retro-reflective markers for the Vicon system were placed on the Velcro suit at the appropriate anatomical locations in accordance with the adapted Plug-in gait specifications. The participant was then fitted with a pair of skates (Bauer Vapor 1X) and were given a pair of gloves (Bauer Nexus) and a Bauer Vapor 95 flex P92 curve stick (Bauer Hockey Ltd., Blainville, Canada). Once the participant was fitted with their appropriate skate size, the Xsens sensors for the feet were placed on the top of the skate boot (roughly the center of where the laces lay) and secured with Gorilla Tape (Gorilla Glue Company, Ohio, USA). The participant was then required to complete the calibration process for both systems, as described in Sections 4.2.1 and 4.2.2. Subsequently, the participant was given time to warm-up and get accustomed to the synthetic ice surface by taking practice shots on the net. Once the warm-up was complete, the Xsens system was calibrated once more prior to the start of testing.

Table 2 Required anthropometric measurements for the respective biomechanical models of motion capture system.

Vicon Plug-In Gait Model	Xsens MVN Link Model
Height	Height
Mass	Foot Length
Ankle Width	Ankle Height
Knee Width	Sole Height
Leg Length	Knee Height
Hand Thickness	Hip Height
Wrist Width	Hip Width
Elbow Width	Arm Span
Shoulder Offset	Shoulder Width
Shoulder Width	Shoulder Height

Each participant performed 10 static standing wrist shots and 10 static standing slap shots for a total of 20 shots. Trials were recorded by both motion capture systems simultaneously. The two systems were synchronized using the Xsens MVN Awinda Station (Xsens, Enschede, Netherlands) at the start of recording, allowing both systems to capture the exact same movements in the same time. For each trial, the puck was placed approximately 5 m from the center of the net. At the beginning of each trial, participants stood adjacent to the puck and did not skate into the shot. Once instructed to begin, the participants were asked to aim at a 0.3 m diameter circular target suspended from the crossbar, then shoot the puck at maximum velocity and accuracy. Additionally, participants were asked to shoot like they normally would in a game and did not receive specific instructions with respect to their technique. Shot trials were divided into one test block of 10 wrist shots and one test block of 10 slap shots. Test order was randomized between participants. In between testing blocks, a brief rest period was provided and the Xsens system was re-calibrated.

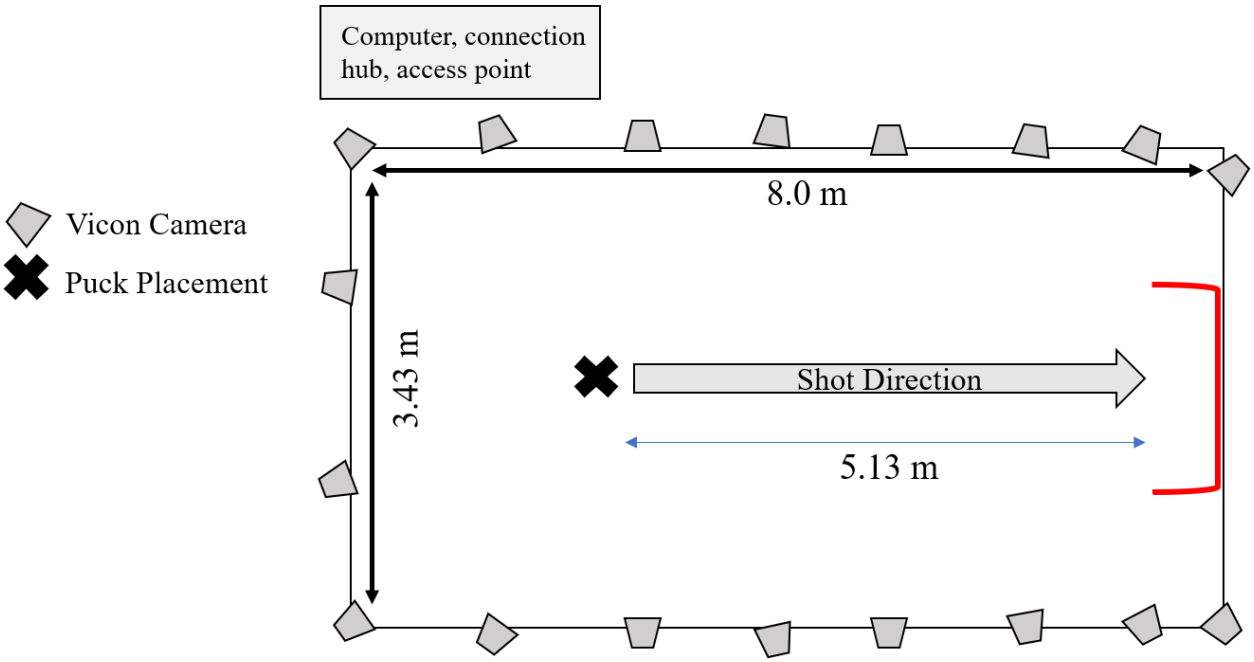

Figure 4 Layout of the in-lab data collection set-up.

4.4 Data Analysis

4.4.1 Data Processing

Data captured using the Vicon cameras was processed using Vicon Nexus 2.6 software. Processing consisted of marker data identification ("labelling") and gap filling (interpolating missing marker positions). This "processed" data from the Nexus software were then imported into Visual3D software (Ver 5.01.23, C-Motion, Germantown, USA) where data were filtered using a 4th order Butterworth filter with a cut-off frequency of 25 Hz and all 3D calculations and event detections were performed. With respect to the data captured using the Xsens system, this data were processed using the built-in Xsens MVN Analyze software (Xsens, Enschede, Netherlands) while joint angles were imported in Matlab R2018b software (Mathworks, Natick, MA, USA). Through the use of the biomechZoo toolbox (Dixon, Loh, Michaud-Paquette, & Pearsall, 2017), shot events were verified and data was organized and normalized.

4.4.2 Joint Kinematic Variables

The MVN Link joint angle data were compared to their respective data from Vicon \ Visual 3D during the two static shooting tasks. Joint angles were measured for the ankle, knee, hip and shoulder joints of both sides, as well as the head and trunk. The elbow and wrist joints were excluded due to the presence of hockey gloves covering the wrists, reducing the accuracy of elbow and wrist kinematics captured by the Vicon system. The selected variables were consistent with the variables measured by Michaud-Paquette et al. (2011).

4.4.3 Joint Angle Calculations

Joint angles calculated with Vicon \ Visual3D data served as the reference angles ("gold standard") for comparison with the Xsens angles. Joint center locations were estimated using anatomical landmarks and anthropometric measurements. Joint angles for the ankle, knee and hip were defined by XYZ rotation, consistent with the joint coordinate systems described by G. Wu et al. (2005) and Grood and Suntay (1983). X-rotation was defined as flexion (+) and extension (-), while Y-rotation was defined as adduction (+) and abduction (-) and Z-rotation was defined as internal rotation (+) and external rotation (-). Similarly, head angles were measured with respect to XYZ rotation around the thorax where X-rotation was defined as extension (+) and flexion (-), Y-rotation was defined as side flexion (right +/left -) and Z-rotation was defined as rotation (left +/right -). Trunk angles were defined by YXZ rotation with respect to the pelvis where X-rotation was defined as extension (+) and flexion (-), Y-rotation was defined as side flexion (right +/left -) and Z-rotation was defined as rotation (left +/right -). Finally, shoulder angle calculations used a Z-Y-Z rotation sequence, in accordance with the ISB recommendations and G. Wu et al. (2005). Consistent with the C-Motion Plug-In Gait guidelines, the shoulder joint centre was inferior to the acromion marker by a distance combining the measured shoulder

radius and the marker radius (C-motion, Germantown, USA). X-rotation was defined as horizontal abduction where 0° was abduction and 90° was forward flexion. Y-rotation was defined as rotation about the humerus Y-axis where negative values represent elevation. Lastly, Z-rotation was defined as internal (+) and external (-) rotation.

With respect to the Xsens MVN system, joint angles followed ISB calculation recommendations (H. Schepers et al., 2018). Kinematic measurements require "sensor-to-segment calibration" and anthropometric measurements in order to track segment orientations (H. Schepers et al., 2018). When calculating joint angles, Xsens uses a coordinate frame with the Y-axis aligned with the vertical, the X-axis pointing forward and the Z-axis pointing laterally. The difference in orientations between the distal and proximal segments is determined when calculating joint angles. The resulting difference is a quaternion that then undergoes Euler angle conversion in accordance with guidelines set by ISB and Grood and Suntay (1983). Joint angles are then calculated using the ZXY sequence where Z-rotation is defined as flexion/extension, X-rotation is defined as abduction/adduction and Y-rotation is defined as internal and external rotation. The "C1/Head" joint was used to define the head, while the Pelvis/T8 joint was used to define the trunk. It should be noted that this sequence of rotations is the same as that for most joints calculated using the Plug-In Gait model in Visual3D, with the exception of axis names. Subsequently, the axes in the Xsens MVN system were re-named to correspond with the Vicon system data where X-rotation represents flexion/extension, Y-rotation represents abduction/adduction and Z-rotation represents internal and external rotation. A limitation when using superficial markers and sensors to estimate joint locations and kinematics is the presence of soft tissue artifact which can cause increased error, especially during dynamic tasks.

4.4.4 Event Detection

Signal events were defined in Visual3D, based on the data recorded using the Vicon system, but were applied to both data sets' waveforms recorded by both systems. Events were calculated using the stick and puck markers with respect to the global coordinate system. The global coordinate system was defined where the Z axis was vertical to the synthetic ice surface, with positive Z was towards the ceiling of the lab space. The X-axis was perpendicular to the direction facing the net. Alternatively, the X-axis was parallel to the cross-bar of the net (positive towards the right post). Finally, the Y-axis was the cross-product of Z and X where the midpoint between the net's post was situated on the positive Y-axis in the global coordinate system. Six events in sequence order were defined for the slap shot, while four events were defined for the wrist shot. These events are described in detail in Table 3.

Table 3 Names and descriptions of events for the slap shot and wrist shot.

Shot Type	Event	Description
Slap Shot	DRAW	The global minimum of the B3 marker of the blade in the global Z direction. i.e. the beginning of the backswing
	TOP	The top of the backswing when the B1 marker of the blade was at its highest position along the global Z-axis. i.e. the beginning of the downswing
	GRND	The maximum blade acceleration in the Z direction between the TOP event and the CON event. i.e. when the blade made contact with the ground
	CON	The frame prior to the frame when the velocity of the puck in the Y direction exceeded 5.0 m/s. i.e. when contact was made between the puck and the stick
	REL	The frame when the distance between B3 marker on the blade and the puck exceeded 0.075 m. i.e. when the puck had been "released" and is no longer in contact with the stick
	FOLTHRU	The frame when blade velocity in the Z direction crossed 0, indicating that the stick was heading in the downward direction after the shot was taken. i.e. the start of the follow-through phase of the shot
Wrist Shot	BACK	The final instance when blade velocity in the Y direction passed 0.05 m/s prior to the FOR event. i.e. the frame where the puck was drawn back with the stick just prior to the beginning of forward progression of the puck
	FOR	The frame where the blade begins to accelerate in the positive Y-direction (direction of puck movement) with a minimum threshold of 150 m/s^2. i.e. when the participant began loading the stick and the blade was advancing forward
	REL	The frame when the distance between B3 marker on the blade and the puck exceeded 0.09 m. i.e. when the puck had been "released" and is no longer in contact with the stick
	FOLTHRU	The frame when blade velocity in the Z direction crossed 0, indicating that the stick was heading in the downward direction after the shot was taken. i.e. the start of the follow-through phase of the shot

Additionally, events known as PRE20 and POST20 were defined for both shot types. The PRE20 event was defined as 20 frames prior to the first event. More specifically, the PRE20 event was defined as 20 frames before the DRAW event for the slap shot and 20 frames before

the BACK event for the wrist shot. The POST20 event was defined as 20 frames after the FOLTHRU event occurred and this was consistent between both shot types.

All trials were inspected for completeness, data quality and event placement prior to the statistical analysis. Trials were removed if certain events were unable to be detected in Visual3D; for example, when stick or puck markers had fallen off or went undetected by the Vicon system. Trials were also inspected for dropped frames. It was found that Xsens MVN Awinda Station synchronization resulted in inconsistent discrepancies in the number of frames recorded by the two systems for a given trial. On other occasions, the "stop recording" trigger from the Xsens system did not always trigger the Vicon system to stop recording, resulting in larger discrepancies. As a result, trials with frame discrepancies exceeding three frames (0.0125 sec) were excluded from the analysis.

4.4.5 Data Normalization

. Waveforms were normalized to 101 data points, scaled to 100% of shot execution, with the PRE20 and POST20 events serving as the beginning and end, respectively. The TOP event served as the division event between back and fore swing for the slap shot trials, while the FOR event served as the middle event for the wrist shot trials. The data were also normalized to account for shot side handeness. "Contralateral" and "ipsilateral" replaced "left" and "right" when identifying limb-specific joints. For example, a left-handed participant's left ankle was referred to as their ipsilateral ankle, while their right ankle was referred to as their contralateral ankle and vice versa.

4.5 Statistical Analysis

Root mean square error (RMSE) and the coefficient of multiple correlation (CMC) were used to compare the joint angles in all three planes derived between Vicon and Xsens systems. RMSE was used to identify the differences in joint angle values and CMC was used to evaluate curve similarity between respective joint angle waveforms. Both descriptive statistics were calculated using Matlab R2018b. Additional analysis included assessing the performance of the Xsens system over time. Paired Samples T-tests ($\alpha = 0.05$) were used to analyze the differences in mean RMSE between the first and last trials.

4.5.1 Coefficient of Multiple Correlation

The coefficient of multiple correlation (CMC) is an effective and standard method of evaluating the curve similarity between waveforms (Di Marco et al., 2018; Garofalo et al., 2009; Kadaba et al., 1989). Demonstrated by Kadaba et al. (1989), CMC is a commonly used method to compare time series measures (Di Marco et al., 2018; Garofalo et al., 2009; Lee et al., 2003), including similar studies comparing the waveforms of motion capture technologies (Mayagoitia et al., 2002; Robert-Lachaine et al., 2017b). The CMC calculation returns a value between 0 and 1, with the criteria where:

- CMC < 0.60 indicates “poor similarity”
- 0.60 ≤ CMC < 0.75 indicates “moderate similarity”
- 0.75 ≤ CMC < 0.85 indicates “good similarity”
- 0.85 ≤ CMC < 0.95 indicates “very good similarity”
- 0.95 ≤ CMC< 1.00 indicates “excellent similarity”

(Di Marco et al., 2018; Garofalo et al., 2009)

The CMC formula used in this study is outlined below. The formula was based on the calculations performed by Ferrari et al. (2010), which was an adapted version of the formula demonstrated by Kadaba et al. (1989).

$$CMC = \sqrt{1 - \frac{\sum_{t=1}^{T}\left[\sum_{s=1}^{S}\sum_{f=1}^{F}\left(Y_{tsf} - \bar{Y}_{tf}\right)^2 / TF_g(S-1)\right]}{\sum_{t=1}^{T}\left[\sum_{s=1}^{S}\sum_{f=1}^{F}\left(Y_{tsf} - \bar{Y}_{t}\right)^2 / T\left(SF_g - 1\right)\right]}}$$

T = Trials (number of trials for a given participant)
S = Systems (2 systems: Xsens and Vicon)
F = Frame (101 frames per trial)

In the CMC formula above, Y_{tsf} represents the data point at frame *f* of the waveform for system *s* of trial *t*. $\bar{Y}_{tf}$ represents the mean data point at frame *f* for trial *t*, while $\bar{Y}_t$ represents the grand mean of all frames for the waveforms of both systems for trial *t*. Variables *T*, F_g and *S* are constants where *S* is 2 and F_g is 100. *T* is the number of trials for a specific participant and therefore varied depending on the participant.

Ferrari et al. (2010) also described the calculation of the offset between waveforms where the mean of one waveform was subtracted by the other waveform. Calculating the CMC with this offset included takes into the account the effect of this magnitude offset on overall similarity. If this offset is comparable with a joint's range of motion however, this can lead CMC values to become complex numbers. CMC values were thus recalculated with the removal of the offset, and CMC values increased noticeably (Ferrari et al., 2010). In the current study, the offset between system waveforms was set to zero, removing the effect of the offset on the CMC value and using CMC solely to evaluate curve similarity while RMSE served as a measurement of angle magnitude differences.

5. Results

An RMSE value was calculated for each trial, while CMC values were calculated for each participant. Both RMSE and CMC values were averaged across all participants in the study. RMSE and CMC values were comparable between wrist and slap shots (Tables 4 and 5). In general, the Xsens system's best accuracy (in reference to Vicon measures) were about the X-axis for both wrist shots and slap shots. Lower limb joint measures were more accurate than in the upper body: ankle and knee joint RMSE were less than 10° (except for ipsilateral knee). Hip joints' RMSE were lowest about the Y-axis (less than 7°) and were comparable between the X- and Z-axes. Both contralateral and ipsilateral shoulder joints had large RMSE, particularly about the Z-axis. Higher Shoulder RMSE were also found during the slap shot than the wrist shot. Trunk RMSE values were least in lateral flexion about the Y-axis while those for the head RMSE were least about the Z-axis.

When averaged across all joints (Tables 6 and 7) RMSE were slightly lower about the Y-axis than the X-axis for the slap shot trials, while the opposite was seen for the wrist shot trials. RMSE values were substantially higher in the Z-axis for both shot types. In the tables, below, CMC indicating very good or excellent curve similarity were represented by the green cells. Moderate or good curve similarity was represented by the yellow cells while poor similarity was represented by the red cells. It should be noted that the averages presented below do not capture the inter-subject variability that was observed. On average, ranges of approximately 14° were observed across subjects about the X and Y axes, with higher ranges observed about the Z-axis.

Table 4 Mean RMSE (degrees) and CMC (R) values for all joints during the slap shot trials. RMSE values were averaged across all trials and all participants, while CMC values were averaged across all participants. Missing CMC values indicate complex numbers.

Joint	X		Y		Z	
	RMSE	CMC	RMSE	CMC	RMSE	CMC
Contralateral Ankle	4.9	0.89	5.1	0.82	25.5	0.40
Ipsilateral Ankle	4.2	0.87	5.9	0.75	25.6	0.57
Contralateral Knee	9.7	0.96	9.5	0.86	27.8	0.69
Ipsilateral Knee	6.9	0.95	10.6	0.78	35.2	0.74
Contralateral Hip	15.4	0.97	6.9	0.99	14.1	0.82
Ipsilateral Hip	14.4	0.97	4.9	0.92	19.5	0.76
Contralateral Shoulder	23.9	0.91	25.7	0.57	88.2	-
Ipsilateral Shoulder	19.0	0.93	28.2	0.65	105.5	0.37
Trunk	15.2	0.80	6.6	0.91	13.5	0.96
Head	14.4	0.82	17.9	0.52	10.5	0.98

Table 5 Mean RMSE (degrees) and CMC (R) values for all joints during the wrist shot trials. RMSE values were averaged across all trials and all participants, while CMC values were averaged across all participants. Missing CMC values indicate complex numbers.

Joint	X		Y		Z	
	RMSE	CMC	RMSE	CMC	RMSE	CMC
Contralateral Ankle	4.6	0.89	5.5	0.86	26.6	0.40
Ipsilateral Ankle	4.4	0.92	7.7	0.74	28.9	0.57
Contralateral Knee	9.3	0.96	8.34	0.84	27.6	0.82
Ipsilateral Knee	7.9	0.90	12.5	0.78	35.1	0.59
Contralateral Hip	11.5	0.95	6.4	0.98	13.2	0.84
Ipsilateral Hip	16.4	0.98	5.5	0.84	19.0	0.80
Contralateral Shoulder	14.7	0.83	14.3	0.85	94.8	-
Ipsilateral Shoulder	15.3	0.93	39.3	-	58.8	-
Trunk	13.1	0.91	5.3	0.87	8.9	0.94
Head	20.4	0.80	15.3	0.47	11.2	0.96

Comparing joint angle-time series curves between Vicon and Xsens, CMC values about most joints' X-axes were greater than 0.85, indicating a very good or excellent curve similarity. CMC values were lower about the Y and Z-axes, suggesting good and moderate curve similarity, respectively. These ratings are in accordance with the criteria provided by Garofalo et al. (2009) and Di Marco et al. (2018).

While CMC values in the Y-axis were lower on average, some joint waveforms did exhibit very good or excellent similarity. For example, the contralateral hip joint waveforms, in particular, showed excellent curve similarity with a CMC values of 0.99 and 0.98 during the slap and wrist shots, respectively. While other joints exhibited strong similarity, such as the trunk or contralateral knee, average CMC was brought down by poor curve similarity seen in joints such as the head and shoulder. Finally, CMC values for the rotation waveforms in the Z-axis ranged from poor similarity to good similarity with the exception of the head and the trunk that conversely demonstrated very good or excellent similarity values.

Table 6 Mean RMSE (degrees) and CMC (R) values across all joints.

Shot Type	**X**		**Y**		**Z**	
	Mean RMSE	**Mean CMC**	**Mean RMSE**	**Mean CMC**	**Mean RMSE**	**Mean CMC**
Slap Shot	12.8	0.91	12.1	0.78	36.5	0.70
Wrist Shot	11.8	0.91	12.0	0.80	32.4	0.74

Table 7 Mean RMSE (degrees) and CMC (R) values across all joints with the contralateral and ipsilateral shoulder RMSE excluded.

Shot Type	**X**		**Y**		**Z**	
	Mean RMSE	**Mean CMC**	**Mean RMSE**	**Mean CMC**	**Mean RMSE**	**Mean CMC**
Slap Shot	10.7	0.91	8.4	0.78	21.4	0.70
Wrist Shot	11.0	0.91	8.3	0.80	21.3	0.74

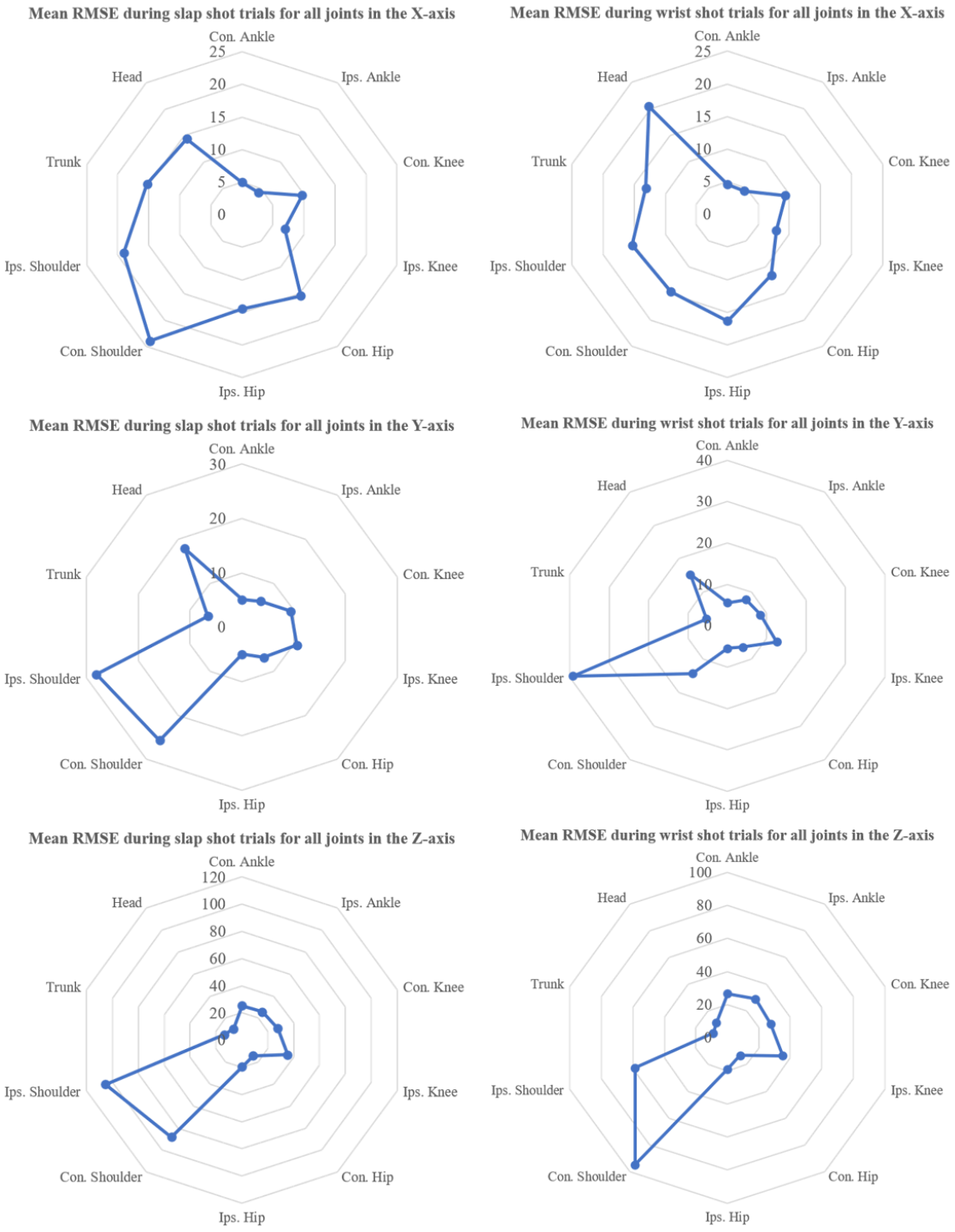

Figure 5 Radar charts displaying Mean RMSE (degrees) values for each joint across all participants. RMSE values are displayed in each axis (Top- X, Middle- Y, Bottom- Z) and for each shot type (Left- Slap, Right- Wrist)

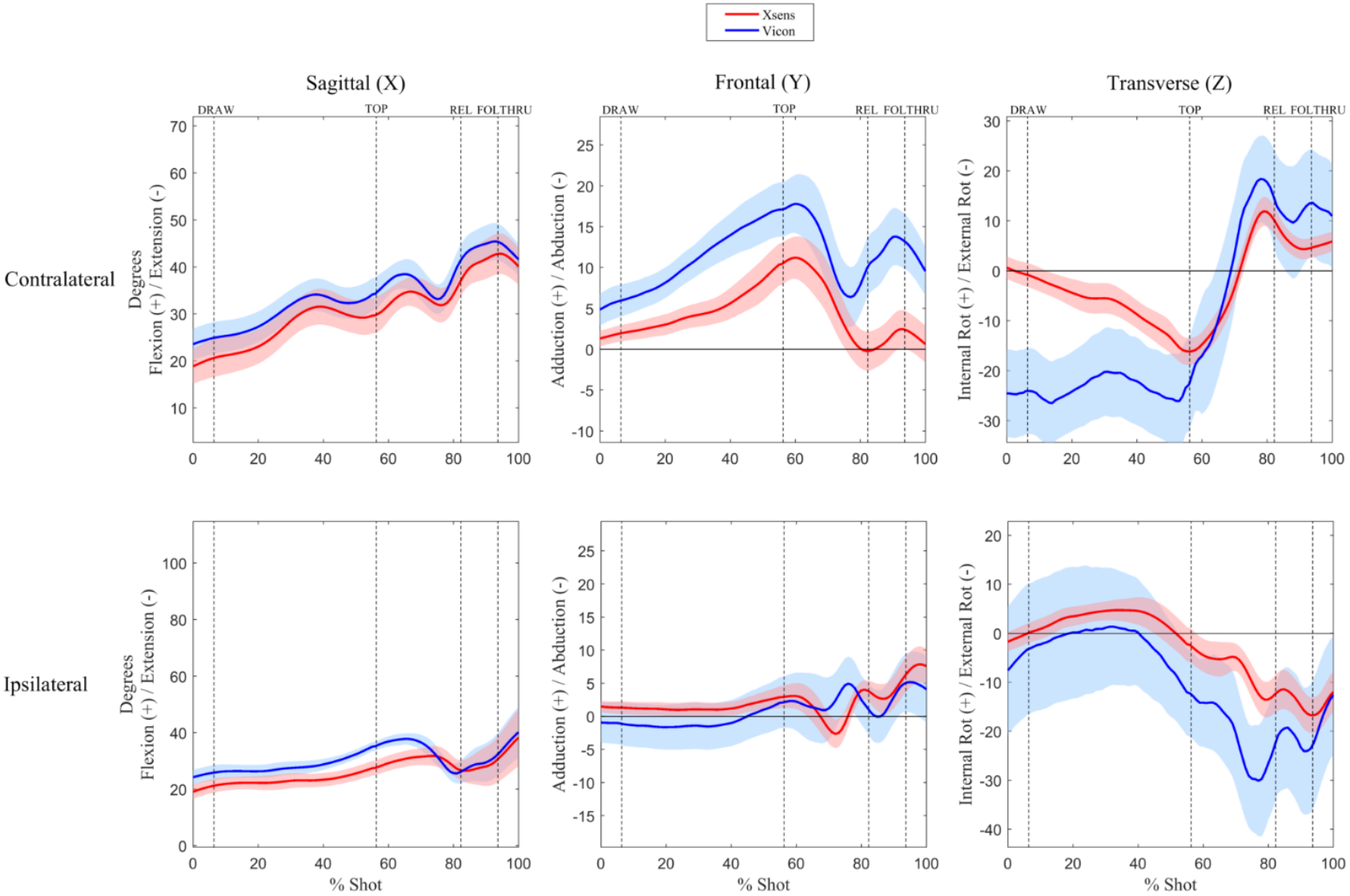

Figure 6 Average knee waveforms of all participants during the slap shot task. Blue waveforms represent Vicon reference data while the red waveforms represent the Xsens data. 95% confidence bands are represented by the coloured bands.

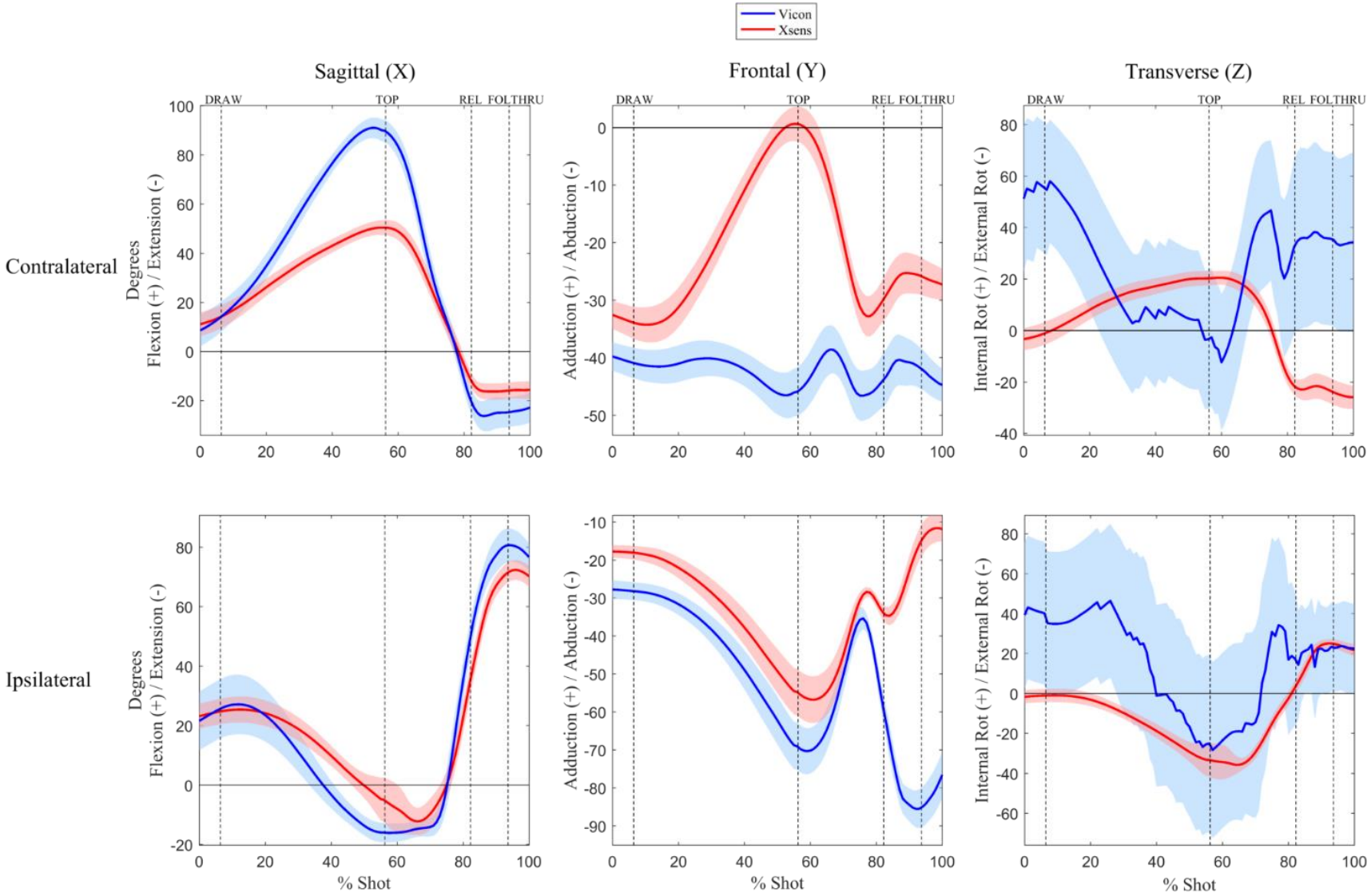

Figure 7 Average shoulder waveforms of all participants during the slap shot task. Blue waveforms represent Vicon reference data while the red waveforms represent the Xsens data. 95% confidence bands are represented by the coloured bands

RMSE values were also compared between the first and last trials as an assessment of system performance (i.e. stability) over time. Paired samples T-tests indicated that there were no significant differences ($\alpha = 0.05$) in RMSE values between the first and last trials across all joints, all axes and both shot types. Mean RMSE values for the two trials are displayed in Tables 8 and 9 where it can be observed that, in some cases, RMSE actually decreased from the first trial to the last. It should be noted that one participant was excluded from this analysis for the slap shot as the first and last trials were removed during the data verification process.

Table 8 Mean RMSE values of participants for each joint during slap shot trials: first and last trials and their differences shown. No significant differences ($p < 0.05$) found.

Joint	**X**			**Y**			**Z**		
	Mean RMSE		**Diff**	**Mean RMSE**		**Diff**	**Mean RMSE**		**Diff**
	First Trial	Last Trial		First Trial	Last Trial		First Trial	Last Trial	
Contralateral Ankle	5.1	5.6	0.5	4.6	5.4	0.8	24.4	25.7	1.3
Ipsilateral Ankle	4.9	4.3	-0.6	6.0	5.5	-0.5	24.3	25.8	1.5
Contralateral Knee	9.7	10.5	0.8	8.8	10.5	1.7	25.7	27.8	2.1
Ipsilateral Knee	7.0	7.0	0.0	10.5	10.5	0.0	33.1	34.0	0.9
Contralateral Hip	15.2	15.9	0.7	6.3	7.5	1.2	14.8	15.4	0.6
Ipsilateral Hip	14.6	14.3	-0.3	4.8	5.3	0.5	19.7	19.2	-0.5
Contralateral Shoulder	22.3	24.6	2.3	24.9	26.8	1.9	87.3	86.1	-1.2
Ipsilateral Shoulder	17.6	18.6	1.0	26.1	29.5	3.4	106.9	101.9	-5.0
Trunk	14.2	15.2	1.0	5.5	6.9	1.4	12.2	14.4	2.2
Head	13.6	14.9	1.3	17.2	18.4	1.2	10.0	10.3	0.3

Table 9 Mean RMSE values of participants for each joint during wrist shot trials: first and last trials and their differences shown. No significant differences ($p < 0.05$) found.

Joint	X			Y			Z		
	Mean RMSE		Diff	Mean RMSE		Diff	Mean RMSE		Diff
	First Trial	Last Trial		First Trial	Last Trial		First Trial	Last Trial	
Contralateral Ankle	4.8	4.6	-0.2	5.3	5.7	0.4	26.1	25.5	-0.6
Ipsilateral Ankle	4.8	4.1	-0.7	7.2	7.7	0.5	30.9	27.1	-3.8
Contralateral Knee	9.8	8.8	-1.0	8.4	8.8	0.4	28.4	26.0	-2.4
Ipsilateral Knee	7.1	7.9	0.8	12.6	12.4	-0.2	34.6	34.7	0.1
Contralateral Hip	11.1	11.9	0.8	6.6	6.7	0.1	12.1	12.8	0.7
Ipsilateral Hip	16.4	16.7	0.3	5.3	5.3	0.0	19.4	19.4	0.0
Contralateral Shoulder	13.3	15.6	2.3	13.0	14.1	1.1	97.4	93.9	-3.5
Ipsilateral Shoulder	15.9	15.2	-0.7	39.9	39.8	-0.1	56.3	60.7	4.4
Trunk	13.2	13.2	1.0	5.5	5.4	-0.1	9.7	9.4	-0.3
Head	19.2	20.8	1.6	14.6	15.5	0.9	10.6	11.2	0.6

6. Discussion

This study examined movement techniques of static ice hockey slap and wrist shot tasks by way of body joint angular movements derived concurrently from two motion capture systems: the Xsens and Xsens MVN model versus the "gold standard" Vicon and an adapted Plug-In Gait model. The purpose of this study was to determine how consistent these angular measures compared between the systems. In general, RMSE of joint angle measures indicated moderate correspondence about the X- and Y-axes (flexion/extension; abduction/adduction) but poor correspondence about the Z-axis (internal/external rotation). There were exceptions: in particular, the shoulder joints showed poor agreement between Vicon/Xsens measures. Trunk RMSE was lowest about the Y-axis, while rotation about the Z-axis yielded the lowest head RMSE. With regards to the hips, agreement varied by axes: good agreement was seen about the Y-axis in contrast to moderate agreement about the X- and Z-axes. This was consistent with the findings of H. Schepers et al. (2018).

On average across all joints, CMC's about the X-axis indicated very good similarity (0.91) between Vicon/Xsens joint angles-time series waveforms, as well as good (0.78-0.80) and moderate (0.70-0.74) curve similarities were seen in the Y- and Z-axis, respectively. This suggests that the Vicon and Xsens systems detected proportionally similar relative joint angular movements throughout the task, despite higher RMSE values. The above results are consistent with those of Wouda et al. (2018) who found lower joint angle differences and higher correlation values in the sagittal plane, while lowest correlation values were found in the Z-axis. H. Schepers et al. (2018) also found slightly lower RMSE's in the sagittal plane compared to the frontal and transverse planes.

Notably the mean RMSE's of all joints and axes were inflated due to the substantial shoulder joint's RMSE, especially in the Z-axis (see Table 7 with adjusted mean RMSE excluding shoulder joints). Removing the shoulder from the sum average would decrease X, Y, Z axes RMSE's by 2°, 4°, and 15°, respectively. In general, shoulder angle measures, particularly about the Z-axis, should be interpreted with additional caution compared to other axes or joints (Figure 7). Inconsistencies in Vicon measurements about the Z-axis may have been the result of soft tissue artefact or the occurrence of collinearity when the upper arms were fully extended (Y. Zhang, Lloyd, Campbell, & Alderson, 2011). Consequently, shoulder rotation about the Z-axis measured by the Xsens system may have been compared to erroneous data and should be interpreted with caution.

Results from other comparative IMU versus optical 3D motion capture studies support the above findings. Kim and Nussbaum (2013) measured the mean and peak average errors (MAE/PAE) for the knee, hip, shoulder and L5/S1 joints. Across three different axes, shoulder joint movement showed the greatest MAE and PAE (less than 6°) for the majority of tasks. In comparison, a study from Luinge, Veltink, and Baten (2007) investigated upper arm orientation during basic tasks commonly performed during morning and eating routines, such as brushing one's teeth. When comparing IMU results to a Vicon reference, Luinge et al. (2007) found errors in orientation of over 40° that were further decreased by incorporating anatomical elbow constraints. The study by Godwin et al. (2009) of upper limb dynamic movements such as washing a table and asymmetric lifting found higher RMSE for upper arm segment orientations compared to other segments including mean Z-axis RMSE of up to 25° and a maximum Z-axis RMSE of 74°. Thus, it was suggested that these RMSE were higher in the non-dominant axes during the movements (Godwin et al., 2009; Kim & Nussbaum, 2013). While the motions

examined by Godwin et al. (2009) are quite different from those examined in the current study, they involved similar rapid changes in direction in upper limb motion. Zhou and Hu (2007) suggested that rapid changes can cause IMUs to "overshoot" their measurements resulting in increases in the calculated error. This may apply to the current study as mean RMSE for the shoulder joints was typically higher during the slap shot than the slower executed wrist shot. Additionally, Robert-Lachaine et al. (2017b) reported that largest shoulder RMSE's occurred between 20 and 40° and was "attributed to differences in the biomechanical models where the joint coordinate system and centre of rotation are not as anatomically comparable, as they are in other joints, between the MVN model and ISB recommendations."

While CMC and RMSE comparisons across joints and axes appear consistent with the literature, the overall magnitude of RMSE was slightly higher in the current study. For example, Robert-Lachaine et al. (2017b) reported lower limb RMSE's within 7° about all three axes. The dynamic nature of the shooting tasks may have contributed to increased error, however, the error between the two systems has primarily been attributed to the sum of differences in their respective technologies and biomechanical models. Robert-Lachaine et al. (2017b) suggested that the error due to technology was relatively minimal, with most error attributed to model differences. As well, differences in upper limb calibration procedures (Xsens' static neutral or T-pose, in contrast to Vicon's static pose: palms down, elbows flexed to 90°, forearms pronated from option 2 of the ISB Recommendations, G. Wu et al. (2005)) may contribute to divergent shoulder joint measures. In summary, though Vicon's kinematic output was posited as the reference gold standard, the measurement (difference) observed between the Vicon and Xsens is largely an artefact of different anatomical models (i.e. a comparison of "apples and oranges",

particularly with respect to the shoulder). Further standardization of joint model definitions is required.

In addition to the above, the accuracy of IMU systems is dependent on the complexity and duration of the tasks measured. Kim and Nussbaum (2013) concluded that greater error was typically associated with the tasks that required larger or whole-body movements. Furthermore, they found accuracy of the Xsens system decreased over time, suggesting a potential temporal effect on system accuracy. Robert-Lachaine et al. (2017b) stated similar conclusions, as RMSE values rose with increased complexity and duration of the task. Similar results were seen in other studies (Brodie et al., 2008; Godwin et al., 2009), while Plamondon et al. (2007) found lower error during shorter tasks compared to longer tasks when measuring trunk posture with an inertial sensor-based system.

Thus, task complexity and duration must be taken into consideration when interpreting results or making comparisons between an IMU system and optoelectronic system, or across different tasks (Brodie et al., 2008; Godwin et al., 2009; Kim & Nussbaum, 2013; Plamondon et al., 2007; Robert-Lachaine et al., 2017b). In the current study, no significant differences were found between mean RMSE from the beginning and end phases of data collection blocks of approximately 10 minutes in length (10 trials per block with re-calibration between blocks). Further study is warranted to determine IMU based measurement accuracy of longer task duration and increased complexity within the context of ice hockey, as well as address how best to adapt biomechanical models (e.g. Vicon Plug-in Gait model when gloves worn) and calibration procedures to yield joint angle measures that end users have confidence in. Additionally, the presence of inter-subject variability should also be investigated in future studies that explore different task complexities and movement patterns during task completion.

This in-lab study's controlled environment yielded high-resolution reference data that demonstrated the feasibility of using Xsens to examine ice hockey tasks. Ultimately, future Xsens based studies can be conducted within ice arenas, to examine skating drills, dynamic shooting drills or a combination of skating and shooting to mimic a game-like scenario over longer time windows. Xsens demonstrated its potential for practical (i.e. real time angle presentation) and less cumbersome data collection than optoelectronic camera-based systems. With further attention to model design and calibration procedures, Xsens joint angle measurement accuracy and/or agreement with other motion capture systems can be improved.

7. Conclusion

The Xsens MVN Link system demonstrated comparable measures to those of the Vicon optoelectronic system. In general, when measuring joint kinematics during slap and wrist shots, low RMSE and high CMC about the X (sagittal) and Y (frontal) axes were observed between the motion captures systems. The RMSE and CMC across different joints and axes were consistent with the literature, though the dynamic nature of the tasks studied may have raised the overall RMSE, especially about the Z (transverse) axis (in particular about the shoulder). While some technological differences in capturing movement and computing angles were expected to contribute to RMSE, it is speculated that a large portion of the calculated difference error between systems was the result of differences in the systems respective biomechanical models and calibration procedures. Finally, no temporal effects (i.e. testing duration) on measurement error were observed over our testing blocks of approximately ten minutes. Future research is thus warranted to evaluate the performance of the Xsens system during longer and more complex, game-like tasks in an ice arena.

References

Ahmadi, A., Mitchell, E., Richter, C., Destelle, F., Gowing, M., O'Connor, N. E., & Moran, K. (2014). Toward automatic activity classification and movement assessment during a sports training session. *IEEE Internet of Things Journal, 2*(1), 23-32.

Ahmadi, A., Rowlands, D. D., & James, D. A. (2010). Development of inertial and novel marker-based techniques and analysis for upper arm rotational velocity measurements in tennis. *Sports Engineering, 12*(4), 179-188.

Bächlin, M., & Tröster, G. (2012). Swimming performance and technique evaluation with wearable acceleration sensors. *Pervasive and Mobile Computing, 8*(1), 68-81.

Baker, R. (2007). The history of gait analysis before the advent of modern computers. *Gait & posture, 26*(3), 331-342.

Bidabadi, S. S., Murray, I., & Lee, G. Y. F. (2018). Validation of foot pitch angle estimation using inertial measurement unit against marker-based optical 3D motion capture system. *Biomedical engineering letters, 8*(3), 283-290.

Brodie, M., Walmsley, A., & Page, W. (2008). Dynamic accuracy of inertial measurement units during simple pendulum motion. *Computer methods in biomechanics and biomedical engineering, 11*(3), 235-242.

Budarick, A. R., Shell, J. R., Robbins, S. M., Wu, T., Renaud, P. J., & Pearsall, D. J. (2018). Ice hockey skating sprints: run to glide mechanics of high calibre male and female athletes. *Sports biomechanics*, 1-17.

De Vries, W., Veeger, H., Baten, C., & Van Der Helm, F. (2009). Magnetic distortion in motion labs, implications for validating inertial magnetic sensors. *Gait & posture, 29*(4), 535-541.

Di Marco, R., Scalona, E., Pacilli, A., Cappa, P., Mazzà, C., & Rossi, S. (2018). How to choose and interpret similarity indices to quantify the variability in gait joint kinematics. *International Biomechanics, 5*(1), 1-8. doi:10.1080/23335432.2018.1426496

Dixon, P. C., Loh, J. J., Michaud-Paquette, Y., & Pearsall, D. J. (2017). biomechZoo: An open-source toolbox for the processing, analysis, and visualization of biomechanical movement data. *Comput Methods Programs Biomed, 140*, 1-10. doi:10.1016/j.cmpb.2016.11.007

Ferrari, A., Cutti, A. G., Garofalo, P., Raggi, M., Heijboer, M., Cappello, A., & Davalli, A. (2010). First in vivo assessment of "Outwalk": a novel protocol for clinical gait analysis based on inertial and magnetic sensors. *Medical & biological engineering & computing, 48*(1), 1.

Fulton, S. K., Pyne, D. B., & Burkett, B. (2009). Validity and reliability of kick count and rate in freestyle using inertial sensor technology. *Journal of sports sciences, 27*(10), 1051-1058.

Garofalo, P., Cutti, A. G., Filippi, M. V., Cavazza, S., Ferrari, A., Cappello, A., & Davalli, A. (2009). Inter-operator reliability and prediction bands of a novel protocol to measure the coordinated movements of shoulder-girdle and humerus in clinical settings. *Med Biol Eng Comput, 47*(5), 475-486. doi:10.1007/s11517-009-0454-z

Ghasemzadeh, H., Loseu, V., & Jafari, R. (2009). Wearable coach for sport training: A quantitative model to evaluate wrist-rotation in golf. *Journal of Ambient Intelligence and Smart Environments, 1*(2), 173-184.

Godwin, A., Agnew, M., & Stevenson, J. (2009). Accuracy of inertial motion sensors in static, quasistatic, and complex dynamic motion. *Journal of biomechanical engineering, 131*(11), 114501.

Grood, E. S., & Suntay, W. J. (1983). A Joint Coordinate System for the Clinical Description of Three-Dimensional Motions: Application to the Knee. *Transactions of the ASME, 105*, 136-144.

Jensen, U., Schmidt, M., Hennig, M., Dassler, F. A., Jaitner, T., & Eskofier, B. M. (2015). An IMU-based mobile system for golf putt analysis. *Sports Engineering, 18*(2), 123-133.

Kadaba, M. P., Ramakrishnan, H. K., Wootten, M. E., Gainey, J., Gorton, G., & Cochran, G. V. B. (1989). Repeatability of Kinematic, Kinetic, and Electromyographic Data in Normal Adult Gait. *Journal of Orthopaedic Research, 7*(6), 849-860.

Kim, S., & Nussbaum, M. A. (2013). Performance evaluation of a wearable inertial motion capture system for capturing physical exposures during manual material handling tasks. *Ergonomics, 56*(2), 314-326.

Koda, H., Sagawa, K., Kuroshima, K., Tsukamoto, T., Urita, K., & Ishibashi, Y. (2010). 3D measurement of forearm and upper arm during throwing motion using body mounted sensor. *Journal of Advanced Mechanical Design, Systems, and Manufacturing, 4*(1), 167-178.

Krüger, A., & Edelmann-Nusser, J. (2010). Application of a full body inertial measurement system in alpine skiing: A comparison with an optical video based system. *Journal of applied biomechanics, 26*(4), 516-521.

Lee, R. Y. W., Laprade, J., & Fung, E. H. K. (2003). A real-time gyroscopic system for three-dimensional measurement of lumbar spine motion. *Medical Engineering & Physics, 25*(10), 817-824. doi:10.1016/s1350-4533(03)00115-2

Lomond, K., Turcotte, R., & Pearsall, D. (2007). Three-dimensional analysis of blade contact in an ice hockey slap shot, in relation to player skill. *Sports Engineering, 10*(2), 87-100.

Luinge, H. J., Veltink, P. H., & Baten, C. T. (2007). Ambulatory measurement of arm orientation. *J Biomech, 40*(1), 78-85. doi:10.1016/j.jbiomech.2005.11.011

Mayagoitia, R. E., Nene, A. V., & Veltink, P. H. (2002). Accelerometer and rate gyroscope measurement of kinematics: an inexpensive alternative to optical motion analysis systems. *Journal of biomechanics, 35*(4), 537-542. doi:10.1016/s0021-9290(01)00231-7

Michaud-Paquette, Y., Magee, P., Pearsall, D., & Turcotte, R. (2011). Whole-body predictors of wrist shot accuracy in ice hockey: a kinematic analysis. *Sports biomechanics, 10*(01), 12-21.

Michaud-Paquette, Y., Pearsall, D. J., & Turcotte, R. A. (2009). Predictors of scoring accuracy: ice hockey wrist shot mechanics. *Sports Engineering, 11*(2), 75-84.

Oatis, C. A. (2017). *Kinesiology: the mechanics and pathomechanics of human movement* (3rd ed.): Wolters Kluwer.

Pearsall, D., Montgomery, D., Rothsching, N., & Turcotte, R. (1999). The influence of stick stiffness on the performance of ice hockey slap shots. *Sports Engineering, 2*, 3-12.

Plamondon, A., Delisle, A., Larue, C., Brouillette, D., McFadden, D., Desjardins, P., & Larivière, C. (2007). Evaluation of a hybrid system for three-dimensional measurement of trunk posture in motion. *Applied Ergonomics, 38*(6), 697-712.

Reenalda, J., Maartens, E., Homan, L., & Buurke, J. J. (2016). Continuous three dimensional analysis of running mechanics during a marathon by means of inertial magnetic measurement units to objectify changes in running mechanics. *Journal of biomechanics, 49*(14), 3362-3367.

Renaud, P. J., Robbins, S. M., Dixon, P. C., Shell, J. R., Turcotte, R. A., & Pearsall, D. J. (2017). Ice hockey skate starts: a comparison of high and low calibre skaters. *Sports Engineering, 20*(4), 255-266.

Robbins, S. M., Renaud, P. J., & Pearsall, D. J. (2018). Principal component analysis identifies differences in ice hockey skating stride between high-and low-calibre players. *Sports biomechanics*, 1-19.

Robert-Lachaine, X., Mecheri, H., Larue, C., & Plamondon, A. (2017a). Accuracy and repeatability of single-pose calibration of inertial measurement units for whole-body motion analysis. *Gait & posture, 54*, 80-86.

Robert-Lachaine, X., Mecheri, H., Larue, C., & Plamondon, A. (2017b). Validation of inertial measurement units with an optoelectronic system for whole-body motion analysis. *Medical & biological engineering & computing, 55*(4), 609-619.

Schepers, H., Giuberti, M., & Bellusci, G. (2018). Xsens MVN: Consistent Tracking of Human Motion Using Inertial Sensing. In *Xsens Technologies* (pp. 1-8).

Schepers, H. M., & Veltink, P. H. (2010). Stochastic magnetic measurement model for relative position and orientation estimation. *Measurement science and technology, 21*(6), 065801.

Seaman, A., & McPhee, J. (2012). Comparison of optical and inertial tracking of full golf swings. *Procedia engineering, 34*, 461-466.

Shell, J. R., Robbins, S. M., Dixon, P. C., Renaud, P. J., Turcotte, R. A., Wu, T., & Pearsall, D. J. (2017). Skating start propulsion: Three-dimensional kinematic analysis of elite male and female ice hockey players. *Sports biomechanics, 16*(3), 313-324.

Taylor, L., Miller, E., & Kaufman, K. R. (2017). Static and dynamic validation of inertial measurement units. *Gait & posture, 57*, 80-84.

van der Kruk, E., & Reijne, M. M. (2018). Accuracy of human motion capture systems for sport applications; state-of-the-art review. *European journal of sport science, 18*(6), 806-819.

van der Kruk, E., Schwab, A., Van Der Helm, F., & Veeger, H. (2016). Getting the Angles Straight in Speed Skating: A Validation Study on an IMU Filter Design to Measure the Lean Angle of the Skate on the Straights. *Procedia engineering, 147*, 590-595.

Villaseñor, A., Turcotte, R., & Pearsall, D. (2006). Recoil effect of the ice hockey stick during a slap shot. *Journal of applied biomechanics, 22*(3), 202-211.

Whiteside, D., Deneweth, J. M., Bedi, A., Zernicke, R. F., & Goulet, G. C. (2015). Femoroacetabular Impingement in Elite Ice Hockey Goaltenders: Etiological Implications of On-Ice Hip Mechanics. *Am J Sports Med, 43*(7), 1689-1697. doi:10.1177/0363546515578251

Worobets, J., Fairbairn, J., & Stefanyshyn, D. (2006). The influence of shaft stiffness on potential energy and puck speed during wrist and slap shots in ice hockey. *Sports Engineering, 9*(4), 191-200.

Wouda, F. J., Giuberti, M., Bellusci, G., Maartens, E., Reenalda, J., Van Beijnum, B.-J. F., & Veltink, P. H. (2018). *On the validity of different motion capture technologies for the analysis of running.* Paper presented at the 2018 7th IEEE International Conference on Biomedical Robotics and Biomechatronics (Biorob).

Wu, G., van der Helm, F. C., Veeger, H. E., Makhsous, M., Van Roy, P., Anglin, C., . . . International Society of, B. (2005). ISB recommendation on definitions of joint coordinate systems of various joints for the reporting of human joint motion--Part II: shoulder, elbow, wrist and hand. *J Biomech, 38*(5), 981-992. doi:10.1016/j.jbiomech.2004.05.042

Wu, T.-C., Pearsall, D., Hodges, A., Turcotte, R., Lefebvre, R., Montgomery, D., & Bateni, H. (2003). The performance of the ice hockey slap and wrist shots: the effects of stick construction and player skill. *Sports Engineering, 6*(1), 31-39.

Xsens. (2018). Xsens MVN User Manual.

Zhang, J. T., Novak, A. C., Brouwer, B., & Li, Q. (2013). Concurrent validation of Xsens MVN measurement of lower limb joint angular kinematics. *Physiol Meas, 34*(8), N63-69. doi:10.1088/0967-3334/34/8/N63

Zhang, Y., Lloyd, D. G., Campbell, A. C., & Alderson, J. A. (2011). Can the effect of soft tissue artifact be eliminated in upper-arm internal-external rotation? *J Appl Biomech*, *27*(3), 258-265. doi:10.1123/jab.27.3.258

Zhou, H., & Hu, H. (2007). Upper limb motion estimation from inertial measurements. *International Journal of Information Technology, 13*(1).